PLISKA
STUDIA MATHEMATICA

ПЛИСКА
МАТЕМАТИЧЕСКИ
СТУДИИ

Pliska Stud. Math. **25** (2015), 155–166

PLISKA
STUDIA MATHEMATICA

2D ELASTODYNAMIC PROBLEMS FOR ANISOTROPIC SOLIDS WITH DEFECTS AT MACRO- AND NANO- SCALE BY INTEGRO-DIFFERENTIAL EQUATIONS

Tsviatko Rangelov, Sonia Parvanova, Petia Dineva

The aim of the study is to propose, develop and validate an accurate and efficient boundary integral equation method (BIEM) and apply it for solution of plane dynamic problems for anisotropic composite solids with cracks, inclusions and holes at macro and nano level. The modeling approach is based on the frame of continuum mechanics, linear wave propagation theory, linear fracture mechanics and surface elasticity theory. The computational tool is displacement and non-hypersingular traction BIEM based on frequency dependent fundamental solution. The obtained results reveal the sensitivity of the dynamic stress concentrations fields to the: (a) type of the defect-crack, hole or inclusion; (b) type of the boundary condition at macro or nano scale; (c) characteristics of the dynamic load; (d) material anisotropy; (e) wave-defect, defect-defect interaction. The non-classical boundary conditions and a localized constitutive equation for the matrix-inclusion interfaces within the framework of the Gurtin-Murdoch surface elasticity theory are developed, applied, and reported for the case of isotropic media. The relevant solid matrix could be an infinite or finite-sized medium containing multiple nano-cavities and/or elastic nano-inclusions of arbitrary shape and configuration.

2010 *Mathematics Subject Classification:* 74J20, 74S15, 74G70.

Key words: Elastodynamics; Macro/nano-holes, inclusions, cracks; General anisotropy; Boundary integral equations; Stress concentration factor; Stress intensity factor.

The authors acknowledge the support of the Bulgarian National Science Fund under the Grant No. DFNI-I 02/12.

The application of the near-field results is in computational fracture mechanics, while the information for the scattered wave field can be used for development of new efficient non-destructive test methods for monitoring of the integrity and reliability of the composite materials and the engineering structures based on them.

1. Introduction

The commonly used computational tools for evaluation of local stress concentrations near defects like cracks, holes and inclusions are the wave function expansion method (Pao and Mow [1]), the integral transform and the singular integral equation method (Ohyoshi [2]), the multi–domain (Dominguez and Gallego [3]), the dual (Abuquerque et al. [4]), the hypersingular (Sladek and Sladek [5]) and the non-hypersingular (Dineva et al. [6]) boundary integral equation (BIE) techniques. The short literature review shows that most of the investigations are restricted to unbounded solids with a simple scenario and that there exist only a few results for dynamic problems for finite anisotropic solids with different type of defects even at macro-level. There are no any results concerning elastodynamic behaviour of finite anisotropic solids with nano–inclusions. The aim of this study is to propose, to develop, to validate and to use in simulations an efficient BIEM and to apply it for the solution of in–plane dynamic problems of anisotropic finite solids with cracks, inclusions and holes at macro- and nano- scale.

2. State of the problem

In a Cartesian coordinate system $Ox_1x_2x_3$ consider an anisotropic matrix M in a bounded domain $G \in R^3 \cap \{x_3 = 0\}$ containing a set of macro- or nano-heterogeneities $I = \cup I_k \in G$ as cracks, holes and inclusions with the interface boundary between the solid material and heterogeneities denoted by $S = \partial I$.

Macro–heterogeneities are with length scale greater than $10^{-6}m$, while the nano–heterogeneities are objects with at least one dimension falling in the interval $10^{-7}m \div 10^{-9}m$. It is assumed that anisotropic material is of monoclinic type (there exists at least one elastic symmetry plane), because only under this assumption is possible uncoupling of the 3D problem to two–dimensional in–plane and anti–plane ones. Plane strain state, i.e. in–plane wave motion with respect to plane $x_3 = 0$ is considered. In this case the only non–zero field quantities are displacements u_1, u_2 and stresses $\sigma_{11}, \sigma_{12}, \sigma_{22}$. Here all field quantities depend on coordinates $x = (x_1, x_2)$ and frequency ω of the applied harmonic in time mechanical load along the matrix boundary ∂G.

The system of partial differential equation of motion has the following form

$$
(1)\quad \begin{cases} c_{11}u_{1,11} + c_{66}u_{1,22} + 2c_{16}u_{1,12} + c_{16}u_{2,11} + c_{26}u_{2,22} + (c_{12} + c_{66})u_{2,12} \\ +\rho\omega^2 u_1 = 0, \\ c_{16}u_{1,11} + c_{26}u_{1,22} + (c_{12} + c_{66})u_{1,12} + c_{66}u_{2,11} + c_{22}u_{2,22} + 2c_{26}u_{2,12} \\ +\rho\omega^2 u_2 = 0, \end{cases}
$$

where comma means partial differentiation and c_{ij} is the contracted Voigt notation applied to the fourth order stiffness tensor C_{ijkl} with properties $C_{ijkl} = C_{jikl} = C_{ijlk} = C_{klij}$ and $C_{ijkl}g_{kl} > 0$ for any non–zero real symmetric tensor g_{kl}. In the case of orthotropic or transversely isotropic material the following symmetry conditions are satisfied $c_{16} = c_{26} = 0$, while for elastic isotropic case $c_{11} = c_{22} = \lambda + 2\mu$ and $c_{12} = \lambda$, $c_{66} = \mu$, where λ and μ are Lamé constants.

Let us define a local coordinate system (n, l), such that it forms right coordinate system at any point along the interface S , where n is unit normal vector and l is unit tangential vector. The traction t_i at any point x on the line segment with normal vector n is defined as $t_i = \sigma_{ij}n_j$, $\sigma_{ij} = C_{ijkl}u_{k,l}$, $i, j = 1, 2$, where $t_i = t_i^M$, $\sigma_{ij} = \sigma_{ij}^M$, $c_{ij} = c_{ij}^M$ for $x \in S$ with normal $n_i = n_i^M$ and $t_i = t_i^I$, $\sigma_{ij} = \sigma_{ij}^I$, $c_{ij} = c_{ij}^I$ for $x \in S$ with normal $n_i = n_i^I$. Note that $n_i^I = -n_i^M$, where n_i^I and n_i^M are the components of the outward normal vector to S considered as a boundary of the inclusion or matrix, respectively. In order to complete the boundary–value problem we should add the boundary conditions along existing boundaries.

Boundary condition along external boundary ∂G of the finite solid G is as follows:

$$
(2)\qquad t_j^M(x,\omega) = t_j^{M0}(x,\omega), \quad x \in \partial G,
$$

where t_j^{M0} is prescribed traction.

Boundary conditions along the interface S between the finite matrix and nano–inclusions is derived by surface elasticity theory in Gurtin and Murdoch [7]. It is assumed that the interface layer S between the matrix and inclusion is with zero thickness. It is isotropic with surface Lamé constants λ^S and μ^S different from elastic properties of the anisotropic inclusions and finite matrix. Such specific behavior of the interface S is due to the surface stress effect introduced in Gurtin and Murdoch [7]. The surface stress is the summation of the surface residual tension τ_0 under unstrained condition and stress due to the surface elasticity. The introduced surface elasticity phenomenon leads to the following non-classical boundary conditions satisfied in tangential and normal direction along S, see Parvanova et al. [8]

$$\begin{pmatrix} t_1^I + t_1^M \\ t_2^I + t_2^M \end{pmatrix} = -\frac{\tau_0}{\kappa}\begin{pmatrix} n_1 \\ n_2 \end{pmatrix} + T^S \begin{pmatrix} u_1 \\ u_2 \end{pmatrix} \quad \text{on } S, \tag{3}$$

where $T^S = T_1 + \dfrac{\partial}{\partial l}T_2 + \dfrac{\partial^2}{\partial l^2}T_3$ and

$$\begin{aligned} T_1 &= \frac{1}{\kappa^2}N\begin{pmatrix} -\alpha & \tau_0\kappa_{,l} \\ -\alpha\kappa_{,l} & -\tau_0 \end{pmatrix}N', \quad N = \begin{pmatrix} n_1 & -n_2 \\ n_2 & n_1 \end{pmatrix}, \\ T_2 &= N\begin{pmatrix} 0 & -\beta \\ \beta & 0 \end{pmatrix}N', \quad T_3 = N\begin{pmatrix} \tau_0 & 0 \\ 0 & \alpha \end{pmatrix}N', \end{aligned}$$

where $\alpha = \lambda^S + 2\mu^S$, $\beta = \dfrac{1}{\kappa}(\alpha + \tau_0)$, $n_i = n_i^I = -n_i^M$, κ is the curvature radius of the interface boundary S, N' is transpose of matrix N, $\dfrac{\partial}{\partial l}, \dfrac{\partial^2}{\partial l^2}$ are first and second tangential derivatives, $t_k^I = \sigma_{kj}^I n_j^I$, $t_k^M = \sigma_{kj}^M n_j^I$. Note that when $\tau_0 = \lambda^S = \mu^S = 0$, the boundary condition (3) transforms into classical boundary condition for traction continuity when there is no jump of stresses from the matrix to inclusion and the surface stress along the interface boundary has negligible effect.

The Boundary Value Problem (BVP) consists of the governing equation (1) and the boundary conditions (2), (3) comprising the following cases for different type of heterogeneities:

(a) nano–inclusions;

(b) nano–holes with $t_j^I = 0$;

(c) macro–inclusions with $\tau_0 = \lambda^S = \mu^S = 0$;

(d) macro–holes with $t_j^I = 0$ and $\tau_0 = \lambda^S = \mu^S = 0$;

(e) macro–cracks with $t_j^I = 0$ and $\tau_0 = \lambda^S = \mu^S = 0$;

(f) nano–cracks with $t_j^I = 0$.

In the present study, in the case of cracks the asymptotic behaviour of displacement and traction near the crack tips is as $u_i = O(\sqrt{r})$ and $t_i = O(1/\sqrt{r})$.

Remark that as the structural dimensions of materials are further scaled down to nanometers, the singular stress field formed near the crack tip is similarly confined to nanometers, where only an extremely smaller number of atoms are present with respect to the macroscale materials. This situation is clearly inconsistent with the fracture mechanics concept based on the continuum theory that postulates the presence of a sufficiently large number of atoms to regard even a crack-tip area as continuum media. Although very few attempts toward this critical issue have been done due to experimental difficulties at the nanometer scale, a result suggested that even a singular stress field of several tens of nanometers would still govern fracture. The discussion for the character of crack-tip singularity contains different and even conflicting opinions. For example, in Sendova and Walton [9] is commented that the crack-tip singularity reduces from the square-root singularity to a logarithmic singularity.

3. BIEM formulation

The defined above BVP can be reformulated via set of the boundary integral equations along the boundaries $S \cup \partial G$ and based on the frequency–dependent fundamental solutions of elastodynamics for in-plane wave motion in generally anisotropic solid containing inclusions and holes at macro- and nano-scale:

$$\begin{aligned} \alpha_{ij}(x)u_i^M(x,\omega) &= -\int_{S\cup\partial G} t_{kj}^{*,M}(x,\xi,\omega)u_k^M(\xi,\omega)d\xi \\ &+ \int_{S\cup\partial G} u_{kj}^{*,M}(x,\xi,\omega)t_k^M(\xi,\omega)d\xi, \quad x\in S\cup\partial G. \end{aligned} \tag{4}$$

$$\begin{aligned} \alpha_{ij}(x)u_i^I(x,\omega) &= -\int_{S} t_{kj}^{*,I}(x,\xi,\omega)u_k^I(\xi,\omega)d\xi \\ &+ \int_{S} u_{kj}^{*,M}(x,\xi,\omega)t_k^I(\xi,\omega)d\xi, \quad x\in S. \end{aligned} \tag{5}$$

In the above, $\alpha_{ij}(x)$ are jump terms dependent on the local geometry at the collocation point $x = (x_1, x_2)$, $u_{ij}^{*,M,I}(x,\xi,\omega)$ is the displacement fundamental solution of the governing equation (1), see Dineva et al. [6], in the matrix or in the inclusion; $t_{ij}^{*,M,I}(x,\xi,\omega) = C_{ijql}u_{qk,l}^{*,M,I}(x,\xi,\omega)n_k$ is the corresponding traction fundamental solution. The displacements and stresses at any point inside the solid can be obtained from the well–known integral representation formulas using the solutions of Eqs. (4) and (5).

The conventional displacement BIEs presented above degenerates for crack problems and cannot be directly applied to crack analysis, see Cruse [10]. There are several methods to overcome this difficulty, among there are: (a) the multi-domain method, see Dominguez and Gallego [3], which introduces artificial boundaries in the elastic body by connecting the crack to a boundary in a way such that each region contains a single crack surface; (b) the single domain approach utilizing a hyper–singular traction BEM, see Sladek and Sladek [5]. More specifically, traction boundary integral equations can be obtained by partial differentiation of the displacement BIE with the subsequent application of the constitutive Hooke's law. This results in a hyper–singular BIE, because of the existence of the spatial derivatives of the stress tensor coming from the displacement fundamental solution. To circumvent this problem involving non–integrable singularities, different regularization techniques have been proposed, see Dineva et al. [6], Sladek and Sladek [5]; (c) the non–hypersingular traction BIE that is based on the conservation integrals of the linear elastodynamics, see Dineva et al. [6]. In the numerical scheme developed here is used the non–hypersingular traction BIEM and the considered BVP for dynamic behavior of an anisotropic solid with cracks is described by the following system of integro–differential equations:

$$\begin{aligned} \alpha_{ij}(x)t_i^0(x,\omega) &= C_{ijkl}n_i(x)\int_{\partial G}\Big[\Big(\sigma^*_{\eta pk}(x,\xi,\omega)u^0_{p,\eta}(\xi,\omega) \\ &- \rho\omega^2 u^*_{pk}(x,\xi,\omega)u^0_p\Big)\delta_{\lambda l} - \sigma^*_{\lambda pk}(x,\xi,\omega)u^0_{p,l}(\xi,\omega)\Big]n_\lambda(\xi)d\xi \\ &- C_{ijkl}n_i(x)\int_{\partial G}u^*_{pk,l}(x,\xi,\omega)t^0_p(\xi,\omega)d\xi, \quad x\in\partial G. \end{aligned} \tag{6}$$

$$\begin{aligned} t_j(x,\omega) &= C_{ijkl}n_i(x)\int_{S}\Big[\Big(\sigma^*_{\eta pk}(x,\xi,\omega)\Delta u^c_{p,\eta}(\xi,\omega) \\ &- \rho\omega^2 u^*_{pk}(x,\xi,\omega)\Delta u^c_p\Big)\delta_{\lambda l} - \sigma^*_{\lambda pk}(x,\xi,\omega)\Delta u^c_{p,l}(\xi,\omega)\Big]n_\lambda(\xi)d\xi \\ &+ C_{ijkl}n_i(x)\int_{\partial G}\Big[\Big(\sigma^*_{\eta pk}(x,\xi,\omega)u^c_{p,\eta}(\xi,\omega) \\ &- \rho\omega^2 u^*_{pk}(x,\xi,\omega)u^c_p\Big)\delta_{\lambda l} - \sigma^*_{\lambda pk}(x,\xi,\omega)u^c_{p,l}(\xi,\omega)\Big]n_\lambda(\xi)d\xi \\ &- C_{ijkl}n_i(x)\int_{\partial G}u^*_{pk,l}(x,\xi,\omega)t^c_p(\xi,\omega)d\xi, \quad x\in\partial G\cup S. \end{aligned} \tag{7}$$

Here $t_j = \begin{cases} \alpha_{ij}t_i^c & \text{on } \partial G \\ -t_j^0 & \text{on } S \end{cases}$, $\sigma^*_{ijm} = C_{ijkl}u^*_{km,l}$, $\Delta u^c_j = u^c_j|_{S^+_{cr}} - u^c_j|_{S^-_{cr}}$, u^0_j, t^0_j denote displacement and traction due to external load on the boundary of the crack free body, while u^c_j, t^c_j are displacement and traction induced by the load $t^c_j = -t^0_j$ on cracks line $S = S^+_{cr}\cup S^-_{cr}$ with zero boundary conditions on ∂G. BIEs (6) and

(7) are integro–differential equations in respect to the unknowns $u_j^0, \Delta u_j^c, u_j^c$. After discretization an algebraic system of equations for the unknowns is obtained and solved. Special crack–tip elements as left quarter point boundary element and right quarter point boundary element are used in order to model in adequately way the asymptotic behavior of displacement and traction near the left and right crack–tips. The regular integrals obtained after discretization are computed employing Gaussian quadrature for one–dimensional integrals and Monte Carlo integration for two–dimensional integrals. The singular integrals are solved analytically utilizing the asymptotic of the fundamental solution for a small argument. Knowing the solution of the algebraic system, the stress–strain field at any point in the solid can be computed by using the integral representation formulas.

The most essential quantities that characterize the non–uniform stress distribution are stress intensity factor (SIF) obtained directly from the traction ahead of the crack–tip and stress concentration factor (SCF) near the inclusion or hole defined as the ratio of the stress along the circumference to the amplitude of the applied load. In case of a straight crack along the interval $(-a, a)$ on the axis Ox_1, the respective formulae for the first and second mode SIFs are: $K_I = \lim_{x_1 \to \pm a} t_2 \sqrt{2\pi(x_1 \mp a)}$ and $K_{II} = \lim_{x_1 \to \pm a} t_1 \sqrt{2\pi(x_1 \mp a)}$.

4. Numerical results for illustrative examples

The first illustrative example is a center cracked elastic orthotropic Boron-epoxy (type I) composite plate $20 \times 40mm$ under uniform uni–axial time–harmonic traction with frequency ω and amplitude $\sigma_0 = 400.106N/m^2$, see Figure 1a, where the boundary conditions are given. The crack–length is $2a = 5mm$. Figure 2 shows K_I^* - SIF-I normalized by $\sigma_0\sqrt{\pi a}$ versus normalized frequency defined as $\Omega = \omega a\sqrt{\rho/c_{66}}$. Figure 2a presents the accuracy of the obtained solution by comparison of the authors' solution with those obtained in Chirino and Dominguez [11] for isotropic material and in Garcia-Sanchez et al. [12] for anisotropic case. In Figure 2b is demonstrated the effect of the orthotropic ratio defined in Garcia-Sanchez et al. [12] as $\varphi = E_1/E_2$, where E_i is the Young's module along i-th coordinate direction. Note that $c_{11} = E_1/(1 - \nu_{12}^2)$, $c_{22} = E_2/(1 - \nu_{12}^2)$, $c_{12} = E_1\nu_{12}/(1 - \nu_{12}^2)$, $c_{66} = \mu_{12}$, $c_{16} = c_{26} = 0$, where ν_{12} is the Poisson's ratio and μ_{12} is the shear modulus. This figure shows that the resonance peak is shifted to lower frequencies with increasing of the orthotropic ratio. The used discretization mesh consists of 20 quadratic boundary elements along the external solid's boundary and 5 quadratic boundary elements along the crack line plus special left and right crack–tip elements near the crack–tips.

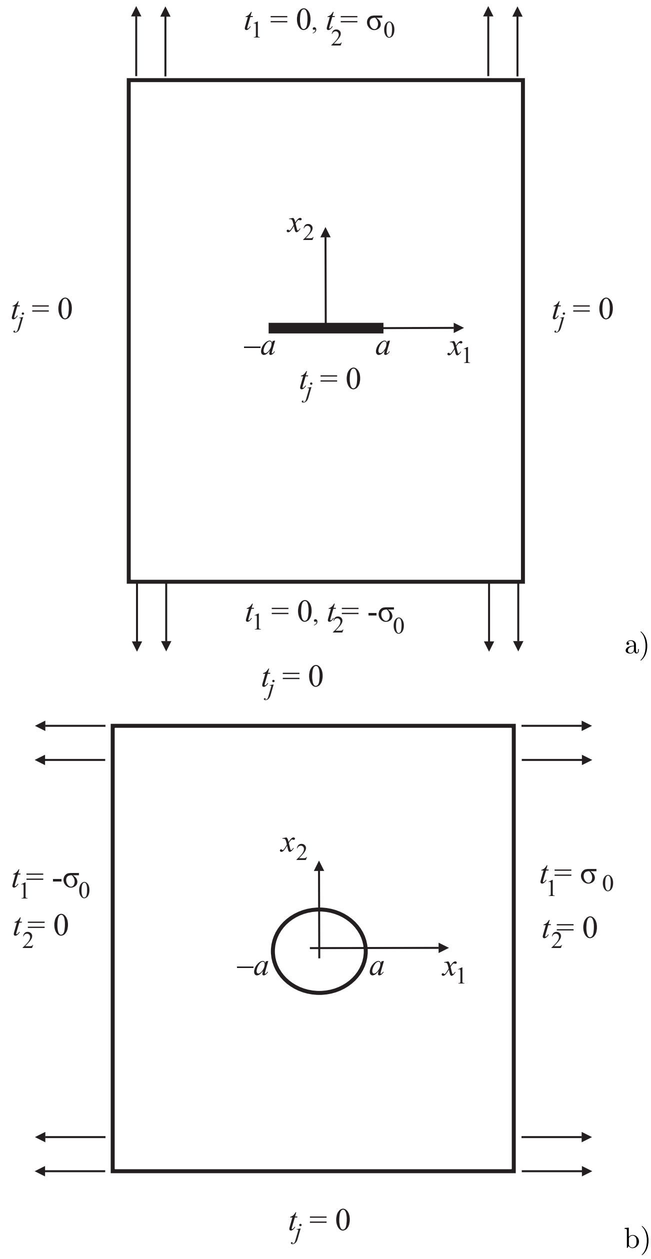

Figure 1: Plate under uniform uni–axial time–harmonic traction: a) A center cracked elastic anisotropic plate at macro–level; b) An elastic isotropic plate with inclusion/hole at nano level

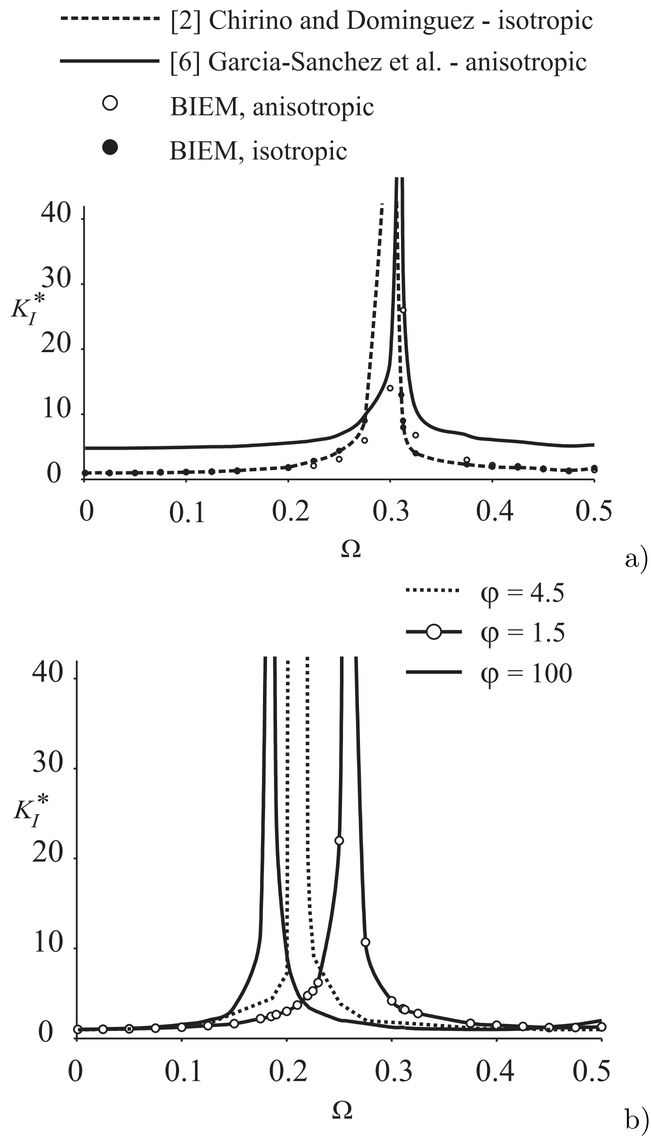

Figure 2: Normalized K_I^* versus frequency for a center cracked Boron epoxy I plate: a) Comparison with results of other authors; b) The effect of the orthotropic ratio φ

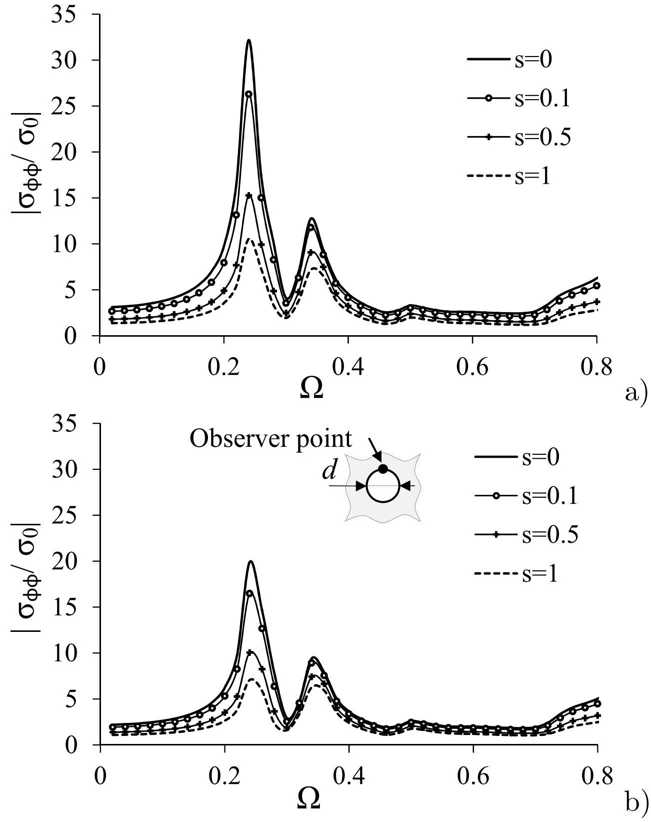

Figure 3: SCF versus frequency at observer point $\phi = \pi/2$ along interface between finite elastic isotropic matrix and: a) Hole; b) Inclusion

The second illustrative example is a square elastic isotropic plate under uniform uni-axial time–harmonic traction of magnitude σ_0 applied to the vertical boundaries, see Figure 1b. The heterogeneity is presented by a circular nano–hole or nano–inclusion with radius a. The size of the square plate is $10d$, where $d = 2a$. A dimensionless parameter is introduced and it is defined as $s = C_S/2\mu^M a$, where μ^M is the shear modulus of the plate material, $C_S = \lambda^S + 2\mu^S$. When the heterogeneity is presented by the inclusion the stiffness ratio of both phases is $\mu^I/\mu^M = 0.2$ and the densities correspond to frequency ratio of $\Omega^I/\Omega^M = 3.0$, where $\Omega^J = \omega a\sqrt{\rho^J/\mu^J}$, $J = I, M$. In all simulations the material damping is set to 5% and Poisson's ratio is 0.26 for both matrix and inclusion. The normalized hoop stresses spectra for representative point with polar angle $\phi = \pi/2$ of the heterogeneity interface versus normalized frequency for a single hole and inclusion cases are plotted in Figure 3. The dynamic SCF is defined as $|\sigma_{\phi\phi}/\sigma_0|$. Four different values of the surface parameter are considered namely $s = 0; 0.1; 0.5; 1.0$. The problem is solved for frequency range up to $\Omega^M = 0.8$. In terms of the discretization, the BEM meshes used to model the perimeter of any given heterogeneity comprised of 32 quadratic boundary elements. The outer boundary of the plate is modeled by 32 equal length boundary elements, 8 along each side.

5. Conclusion

Time–harmonic elastodynamic analysis of anisotropic finite solids with defects such as macro- and nano- sized cracks, inclusions and holes is presented in this work. The mathematical model combines classical 2D elastodynamic theory and surface elasticity model, see Gurtin and Murdoch [7] allowing in such way to treat heterogeneities at both macro and nano level. The analysis is carried out using displacement and non–hypersingular traction BIEM that employed the appropriate frequency–dependent fundamental solution, obtained with Radon transform. The BIEM formulation is implemented numerically by discretization of all defect surfaces using standard collocation schemes. Finally, numerical simulations show that the stress concentration field near defects is strongly influenced by the type and the size of the defect(crack, hole or inclusion), the material anisotropy, the defect location and geometry, the dynamic load characteristics and the mutual interactions between defects and between them and the solid's boundary. The results of the present methodology are with application in the fields of computational fracture mechanics, geotechnical engineering and non–destructive testing evaluation of anisotropic composite materials.

References

[1] Y. H. Pao, C. C. Mow. *Diffraction of elastic waves and dynamic stress concentration.* Crane Russak, New York, 1971.

[2] T. Ohyoshi. Effect of orthotropy on singular stresses for a finite crack. *ASME, J. Appl. Mech.*, **40** (1973b), 491–497.

[3] J. Dominguez, R. Gallego. Time domain boundary element method for dynamic stress intensity factor computations. *Int. J. Num. Methods Eng.*, **33** (1992) No 3, 635–647.

[4] E. L. Abuquerque, P. Sollero, P. Fidelinski. Dual reciprocity boundary element method in Laplace domain applied to anisotropic dynamic crack problems. *Computers and Structures*, **81** (2003), 1703–1713.

[5] J. Sladek, V. Sladek. Transient elastodynamic three–dimensional problems in cracked bodies. *Appl. Math. Model.*, **8** (1984), 2–10.

[6] P. Dineva, D. Gross, R. Müller, T. Rangelov. *Dynamic Fracture of Piezoelectric Materials. Solutions of Time-harmonic problems via BIEM.* Solid Mechanics and its Applications, v. 212, Springer Int. Publ., Switzerland, 2014.

[7] M. E. Gurtin, A. I. Murdoch. A continuum theory of elastic material surfaces. *Arch. Ration. Mach. Anal.*, **57** (1975), 291–323.

[8] S. Parvanova, G. Manolis, P. Dineva. Wave scattering by hahoheterogeneities embedded in a elastic matrix via BEM. *Eng. Anal. Bound. Elem.*, **56** (1915), 57–69.

[9] T. Sendova, J. R. Walton. A new approach to the modeling and analysis of fracture through extension of continuum mechanics to the nanoscale. *Math. Mech. Solids*, **15** (2010), No 3, 368–413.

[10] T. A. Cruse. Two-dimensional BIE fracture mechanics analysis. *Appl. Math. Model.*, **2** (1978), 287–293.

[11] F. Chirino, J. Dominguez. Dynamic analysis of cracks using BEM. *Engng. Fract. Mech.*, **34**, (1989), 1051–1061.

[12] F. Garcia-Sanchez, A. Saez, J. Dominguez. Two-dimensional time-harmonic bem for cracked anisotropic solids. *Engng. Anal. Bound. Elem.*, **30** (2006), 88–99.

Tsviatko Rangelov
Institute of Mathematics
and Informatics
Acad. G. Bonchev Str., Bl. 8
1113 Sofia, Bulgaria
e-mail: `rangelov@math.bas.bg`

Sonia Parvanova
Department of Structural Engineering
University of Architecture,
Civil Engineering and Geodesy
1, H. Smirnenski Blvd
1046 Sofia, Bulgaria
e-mail: `slp_fce@uacg.bg`

Petia Dineva
Institute of Mechanics
Acad. G. Bonchev Str., Bl. 4
1113 Sofia, Bulgaria
e-mail: `petia@imbm.bas.bg`